

# Temperature dependence of magnetic order in single-crystalline UPdSn

R. A. Robinson

LANSCÉ, Los Alamos National Laboratory, Los Alamos, New Mexico 87545

J. W. Lynn

Reactor Radiation Division, National Institute of Standards and Technology, Gaithersburg, Maryland 20899

A. C. Lawson

Materials Science and Technology Division, Los Alamos National Laboratory, Los Alamos, New Mexico 87545

H. Nakotte

Van der Waals-Zeeman Laboratory, University of Amsterdam, 1018 XE, Amsterdam, The Netherlands

The noncollinear hexagonal antiferromagnet UPdSn exhibits two magnetic phase transitions, at 35.5 and 23 K. The first transition is from a hexagonal paramagnetic state to a noncollinear antiferromagnetic state with a doubled unit cell (phase I). The second 23-K transition is to a monoclinic magnetic structure (phase II). Ever since these transitions were discovered, the question has been whether the moments simply rotate at 23 K, or whether the  $y$  and  $z$  components of the moment order at 35.5 K while the  $x$  component orders out of incipient fluctuations at the lower 23-K transition. While previous powder studies were rather inconclusive on this point, in this study new single-crystal neutron-diffraction results are presented that show the second picture to be correct. In addition, the structural distortions that accompany the change in symmetry are discussed and show that there is phase-II type magnetic short-range order between 23 and 35.5 K.

The ternary intermetallic compound UPdSn is one member of the set of 1:1:1 UTX (where T=transition metal, X= $p$ -electron metal) compounds that has been studied for some time now<sup>1-3</sup> with a view to understanding the role of  $f$ - $d$  hybridization in uranium magnetism, and in particular the huge magnetocrystalline anisotropies that are observed. A picture is emerging in which the  $f$  electrons hybridize in directions or planes containing nearest-neighbor U-U links, with the ordered magnetic moments perpendicular to these directions or planes. However, UPdSn does not fit the general pattern and exhibits more localized behavior, as manifested in its low electronic specific heat ( $\gamma_{el}=5$  J mol<sup>-1</sup> K<sup>-2</sup>)<sup>4</sup> and its relatively large ordered moment (2.05  $\mu_B$  at low temperature).<sup>5</sup> The Pd and Sn atoms are ordered chemically in the GaGeLi structure and the uranium ions exhibit a complicated noncollinear magnetic structure with a Néel temperature of 37 K.<sup>5</sup> The original powder-diffraction work<sup>5</sup> on the magnetic structure assumed two magnetic phase transitions, the lower being at 25 K, with a monoclinic noncollinear magnetic structure (phase II, see Fig. 1) below 25 K, an orthorhombic noncollinear magnetic structure (phase I, in which  $\theta=0$  and  $\gamma=90^\circ$ ) between 25 and 37 K and a paramagnetic hexagonal phase above 37 K. Magnetically driven structural distortions with these symmetries have recently been observed and characterized,<sup>6</sup> confirming the original magnetic structure determination. However, there have always been two different ways of regarding the 25-K transition; in a moment-rotation picture, well-defined local moments would start to rotate away from the  $b$ - $c$  plane at 25 K, but there would be no anomalies in the temperature variation of the total uranium moment. Alternatively, the  $y$  and  $z$  components of the moment could order at 37 K, while the  $x$  component ordered at the lower temperature of 25 K. In between,  $\mu_x$  would only be short-range ordered or fluctuating. In this case, there would be a discontinuity in the varia-

tion of the total moment with temperature, so the two pictures should be distinguishable by experiment. In fact a careful temperature-dependent study has already been done on a powder sample,<sup>7</sup> but the results were rather inconclusive. If viewed in spherical-polar coordinates, the order parameters all seem to vary smoothly with no evidence of the 25-K transition. On the other hand, if viewed in Cartesian coordinates, it seems that  $\mu_y$  orders at 37 K or so while  $\mu_x$  orders at 25 K, thereby favoring the idea that  $\mu_x$  condenses at the lower temperature.

Since that study single crystals have been grown and, in the course of a study of the magnetic phase diagram<sup>8</sup> of UPdSn, it was shown that the 010 reflection, whose intensity is proportional to  $\mu_x^2$ , does vary much more sharply with

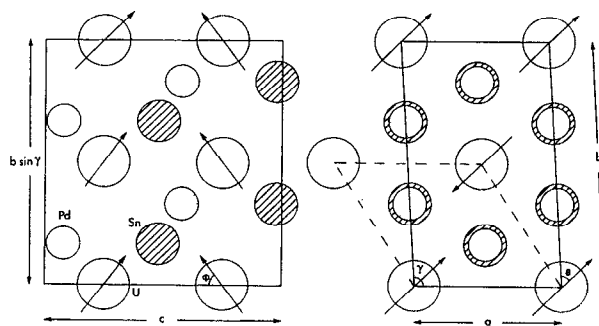


FIG. 1. The crystallographic and magnetic structures at low temperature of UPdSn, with magnetic space group  $P_2112_1$ . The figure on the right shows the monoclinic basal plane. The primitive crystallographic unit cell (which corresponds to the parent hexagonal cell) is shown by the dashed lines, while the magnetic unit cell is shown by the solid lines. The figure on the left shows the projection onto a plane perpendicular to the  $a$  axis. Neither the atom sizes nor the lattice constants are drawn to scale and the deviation from  $90^\circ$  of the monoclinic angle  $\gamma$  has been grossly exaggerated. However, the atom coordinates within the cell are drawn to scale.

temperature than in the powder. In this article, we report new temperature-dependent single-crystal data taken on the 010, 011, 012, 100, and 120 reflections. These give definitive evidence that  $\mu_x$  does indeed condense at the lower temperature of 23 K and that it is short-range ordered or fluctuating between 23 and 35.5 K.

The crystal of UPdSn is the same 1 mm-diam 5-mm-long sample used in previous studies of the magnetic phase diagram<sup>8</sup> and magnetic form factor.<sup>9</sup> It was grown by the tri-arc Czochralski method and for the present experiments was glued into a 1-cm-diam cylindrical aluminum block. The cylinder axis of the crystal was approximately 18° away from the  $[110]_{\text{hexagonal}}$  ( $= [100]_{\text{orthorhombic}}$ ) axis which was aligned along the axis of the aluminum block. This was installed in a closed-cycle helium refrigerator, which was mounted on the BT-4 triple-axis spectrometer at the NIST Research Reactor. A pyrolytic graphite monochromator and filter were used with an incident neutron wavelength  $\gamma = 2.35$  Å and the analyzer was removed. For most of the data presented here, the collimation was 40'/40'/40', but both coarser (40'/40'/open) and tighter (60'/20'/20' and 20'/20'/10') collimations were used in the specific instances noted in some of the figures. Two different crystal orientations were used; (a) with the  $[100]$  orthorhombic axis vertical, giving access to the 010, 011, and 012 reflections of one particular domain pair, and (b) the  $[001]$  axis giving access to the 010, 120, and 100 reflections of the same domain pair. As the cylinder axis of the sample is close to vertical in the first geometry, corrections for self-absorption are a minimum in this case and will be similar for the 010, 011, and 012 reflections. In contrast, with the  $[001]$  axis vertical such corrections will be much larger and more variable from reflection-to-reflection. We have, therefore, only used the 010, 011, and 011 reflections to determine the model parameters  $\mu$ ,  $\theta$ , and  $\phi$  in the magnetic structure of UPdSn.

The temperature variations of the peak intensities of all reflections measured are shown in Fig. 2. The peak widths were also measured at a limited sample of these temperatures for each reflection and, except for the case of the 100 reflection, were found to be temperature independent. There is evidence in these scans of two transitions and we extract transition temperatures of 23 and 35.5 K. These values are in reasonable agreement with previous results.

In the case of the 100 reflection, full peak scans were also made in order to measure the integrated intensities and the results are shown in Fig. 3. These results are very different from the peak intensities in Fig. 2(e) and the reason is that the peak width increases dramatically below 23 K. The inset to Fig. 3 shows peak widths of rocking curves measured with very high angular resolution. This broadening is due to the structural transformation, i.e., orthorhombic to monoclinic, that accompanies the magnetic transition from phase I to phase II.<sup>6</sup> The monoclinic angle  $\gamma$  has previously been determined to be 90.35°, by means of high-resolution neutron powder diffraction.<sup>6</sup> No splitting between the two monoclinic domains was observed, but the angular distribution is broad and flat-topped with a width of approximately 0.8° full width at half-maximum (FWHM). This is qualitatively consistent with having both monoclinic domains and

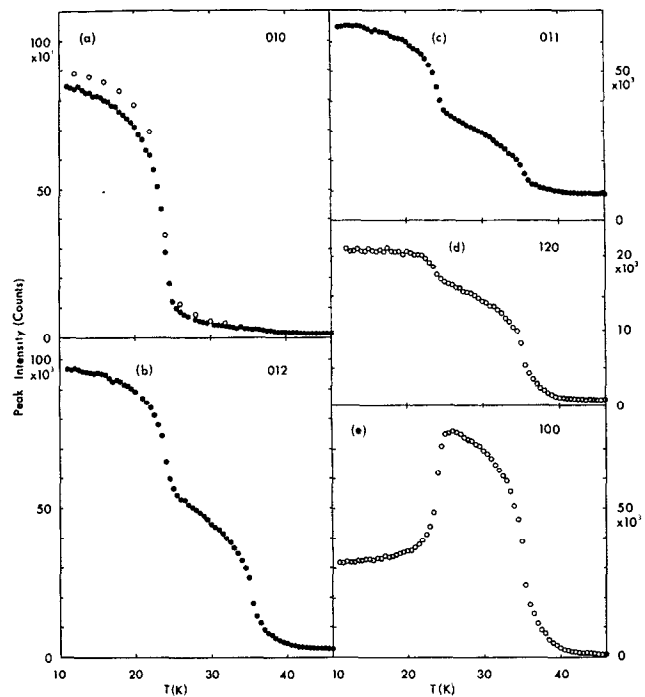


FIG. 2. The variation in peak intensity with temperature for the following magnetic Bragg reflections: (a) 010, (b) 012, (c) 011, (d) 120, and (e) 100. All data are for the magnetic domain (or pair of domains in the low-temperature monoclinic phase) and 40'/40'/40' collimation was used in all cases. The solid circles represent data taken with the  $[100]$  orthorhombic axis vertical, while the open circles represent data taken with the  $[001]$  axis vertical. The data were counted for 5 min per point except for the solid circles in (a) which were counted for 3 min per point. These single crystal data are directly comparable with the powder results in Fig. 4 of Ref. 7.

the consequent angular spread of 0.7° between them, but with a large population of domains in each orientation and a continuous distribution of orientations to accommodate the strains that are induced by the transformation.

We therefore believe that, apart from the 100 reflection, the peak intensities are proportional to the integrated intensity that one would measure in a rocking-curve measurement. The intensity of the 010 reflection shown in Fig. 2(a) is much as reported previously, for this single crystal.<sup>8</sup> There is also clear evidence of two transitions in Figs. 1(b)–(d). Indeed it is almost inconceivable that simple moment rotation could give rise to the step rise at approximately 23 K. In order to demonstrate this point definitively, the intensities of the 010, 011, and 012 reflections were fitted to the model of the magnetic structure shown in Fig. 1. The high-temperature background, derived from data points with temperatures greater than 42 K, was subtracted from the data and the intensities were corrected for the difference in counting time, the  $1/\sin \theta$  Lorentz factor as is appropriate for integrated intensities of rocking curves<sup>10</sup> and the  $U^{3+}$  magnetic form factor.<sup>9</sup> The model parameters  $\mu$ ,  $\theta$ , and  $\phi$  were then treated as adjustable variables and the results are shown as the solid circles in Fig. 4. The rise in total moment at 23 K is clear evidence that the moments are not simply rotating. An extra component seems to be condensing at this temperature. The open circles in Fig. 4 represent simply the component of the

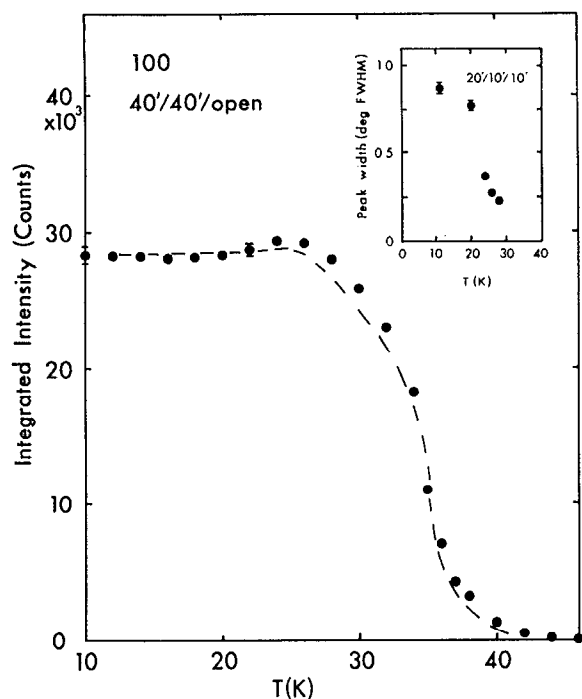


FIG. 3. The variation in integrated intensity for rocking curves through the 100 magnetic reflection, as a function of temperature. The solid circles are the raw data and the dashed line is calculated from the model parameters displayed in Fig. 4, which were in turn derived from the peak intensities of the 010, 011, and 012 reflections as displayed in Fig. 2. The inset shows the variation in peak width with temperature for the same 100 reflection measured with  $20^\circ/10^\circ/10^\circ$  collimation.

moment in the  $b$ - $c$  plane and this is fairly well behaved at 23 K. The small glitch there may be evidence of coupling between moments in the  $b$ - $c$  plane and those perpendicular ( $\mu_x$ ) to it, but the basic picture for this material is that the in-plane moments condense at 35.5 K with  $\mu_x$  condensing at the lower transition. Now, the integrated intensity of the 100 reflection is simply proportional to  $\mu_y^2$  and we can, therefore, calculate the intensity of the 100 reflection at all temperatures from the values of  $\mu_y$ . Suitably scaled to the lowest-temperature-measured integrated intensity, these results are shown as the dashed line in Fig. 3. The agreement between these results, which were derived from the peak intensities of the 010, 011, and 012 reflections are in very good agreement with our direct measurements of integrated intensities for the 100 reflection.

In summary, the main result of this article is shown in the lowest panel of Fig. 4, which shows definitively that the 23-K transition in UPdSn is best thought of as due to condensation of a long-range ordered  $\mu_x$  out of short-range magnetic order in this coordinate between 23 and 35.5 K. In UPdSn, we are not dealing with simple rotation of local moments. In addition, we have observed a large orientational broadening in the single crystal, which is consistent with the monoclinic structural distortion previously observed by powder diffraction.

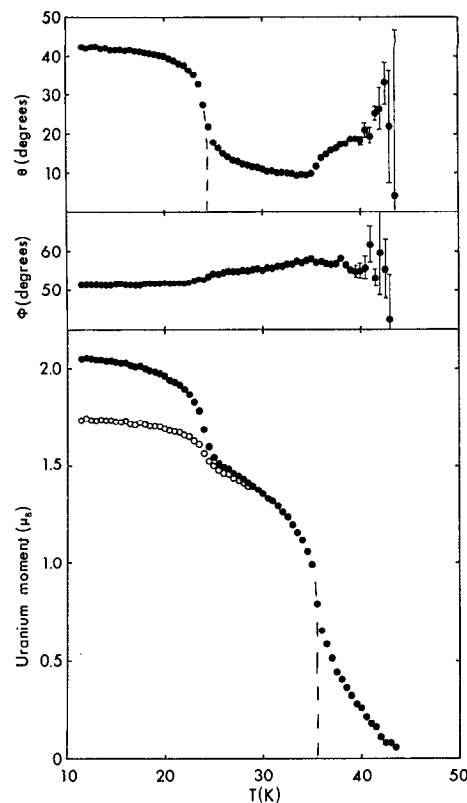


FIG. 4. The variation of model parameters  $\mu$ ,  $\theta$ , and  $\phi$ , with temperature as extracted from the 010, 011, and 012 peak intensities from Fig. 2. These single-crystal data are directly comparable with the powder results in Fig. 3 of Ref. 7. The dashed lines are guides to the eye and have no theoretical significance.

We are grateful to M. F. Collins, who originally suggested to us that the 25-K transition might be better thought of as due to the  $x$ -component ordering at a lower temperature than the components in the  $b$ - $c$  plane. This work was supported in part by the division of Basic Energy Sciences of the U.S. Department of Energy.

- <sup>1</sup> T. T. M. Palstra, G. J. Nieuwenhuys, R. F. M. Vlastuin, J. van den Berg, J. A. Mydosh, and K. H. J. Buschow, *J. Magn. Magn. Mater.* **67**, 331 (1987).
- <sup>2</sup> V. Sechovsky, L. Havela, H. Nakotte, F. R. de Boer, and E. Brück, *J. Alloys Compounds* (to be published).
- <sup>3</sup> R. A. Robinson, A. C. Lawson, V. Sechovsky, L. Havela, Y. Kergadallan, and H. Nakotte, *J. Alloys Compounds* (to be published).
- <sup>4</sup> F. R. de Boer, E. Brück, H. Nakotte, A. V. Andreev, V. Sechovsky, L. Havela, P. Nozar, C. J. M. Denissen, K. H. J. Buschow, B. Vaziri, P. Meissner, H. Maletta, and P. Rogl, *Physica B* **176**, 275 (1991).
- <sup>5</sup> R. A. Robinson, A. C. Lawson, K. H. J. Buschow, F. R. de Boer, V. Sechovsky, and R. B. Von Dreele, *J. Magn. Magn. Mater.* **98**, 147 (1991).
- <sup>6</sup> R. A. Robinson, A. C. Lawson, J. A. Goldstone, and K. H. J. Buschow, *J. Magn. Magn. Mater.* **128**, 143 (1993).
- <sup>7</sup> R. A. Robinson, A. C. Lawson, J. W. Lynn, and K. H. J. Buschow, *Phys. Rev. B* **45**, 2939 (1992).
- <sup>8</sup> H. Nakotte, R. A. Robinson, J. W. Lynn, E. Brück, and F. R. de Boer, *Phys. Rev. B* **47**, 831 (1993).
- <sup>9</sup> S. W. Johnson, R. A. Robinson, H. Nakotte, E. Brück, F. R. de Boer, and A. C. Larson, *J. Appl. Phys.* **73**, 6072 (1993).
- <sup>10</sup> G. L. Squires, *Introduction to the Theory of Thermal Neutron Scattering* (Cambridge University Press, Cambridge, 1978), pp. 41–42.